1. Roy Eason

E82-10376

2. # AgRISTARS

7. SM-J0-00470
JSC-16372
NASA-TM-84852

A Joint Program for Agriculture and Resources Inventory Surveys Through Aerospace Remote Sensing

Soil Moisture

6. October 1980
5. NAS 9-15800

A PARAMETRIC STUDY OF TILLAGE EFFECTS ON RADAR BACKSCATTER

3 R. G. Fenner and G. F. Pels
National Aeronautics and Space Administration
Houston, Texas 77058

S. C. Reid
4. Lockheed Engineering and Management Services Company, Inc.
Houston, Texas 77058

(E82-10376) A PARAMETRIC STUDY OF TILLAGE EFFECTS ON RADAR BACKSCATTER (NASA) 34 p HC A03/MF A01 CSCL 20N

N82-32798

Unclas
G3/43 00376

Lyndon B. Johnson Space Center
Houston, Texas 77058

Dis
Acc

only copy

1. Report No. JSC-16372/ SM-J0-00470

2. Government Accession No.

3. Recipient's Catalog No.

4. Title and Subtitle

A PARAMETRIC STUDY OF TILLAGE EFFECTS ON RADAR BACKSCATTER

5. Report Date October 1980

6. Performing Organization Code ED6

7. Author(s)

Richard G. Fenner, Gerald F. Pels, and Stephen C. Reid

8. Performing Organization Report No.

9. Performing Organization Name and Address

National Aeornautics and Space Administration
Lyndon B. Johnson Space Center
Houston, Texas 77058

Lockheed Engineering and Management Services Company, Inc.
1830 NASA Road 1
Houston, Texas 77058

10. Work Unit No.

11. Contract or Grant No.

12. Sponsoring Agency Name and Address

National Aeornautics and Space Administration
Lyndon B. Johnson Space Center
Houston, Texas 77058

13. Type of Report and Period Covered Technical Report

14. Sponsoring Agency Code

15. Supplementary Notes

16. Abstract

The effects of tillage or ground preparation have been observed in radar imagery for many years. Imagery taken over farming areas frequently shows fields whose brightness is a direct function of the direction of the rows. Analysis of airborne radar backscatter data being gathered for the NASA Agriculture Soil Moisture Experiment (ASME) indicated that tillage, particularly in bare or sparsely vegetated fields, had a large effect which could not be ignored when performing detailed data analysis for soil moisture signatures. To better understand this effect, the NASA/Johnson Space Center, Experiment Systems Division initiated a quantitative investigation of this effect using ground and airborne scatterometer systems in 1978. After studying the data from the 1978 field measurements, the JSME (Joint Soil Moisture Experiment) members requested that the investigation be expanded into a parametric study of various field configurations.

This paper presents the results to date from this investigation. Radar backscatter data for the different field configurations and modulation function curves for angular and frequency variations are presented. A simplistic approach to modeling this effect is presented.

17. Key Words (Suggested by Author(s))

Tillage effects on radar backscatter

18. Distribution Statement

19. Security Classif. (of this report)	20. Security Classif. (of this page)	21. No. of Pages	22. Price*
Unclassified	Unclassified	32	

*For sale by the National Technical Information Service, Springfield, Virginia 22161

JSC Form 1424 (Rev Nov 75)

NASA — JSC

SM-J0-00470
JSC-163721

A PARAMETRIC STUDY OF TILLAGE EFFECTS ON RADAR BACKSCATTER

BY

Richard G. Fenner
NASA/Johnson Space Center
Houston, Texas 77058
(713) 483-3073

Gerald F. Pels
NASA/Johnson Space Center
Houston, Texas 77058
(713) 483-3071

Stephen C. Reid
Lockheed Engineering and
Management Services Company, Inc.
1830 NASA Road One
Houston, Texas 77058
(713) 483-2191

JANUARY 1980

1.0 INTRODUCTION

The effects of tillage on ground preparation have been observed for many years. Porcello and Rendleman[1] first mentioned this effect in analyses of imagery taken over a Garden City, Kansas agricultural test site in 1972.

The effects of tillage were further investigated by Ulaby and Batlivala in 1975[2] and Ulaby and Bare in 1978[3]. These studies used the Garden City, Kansas imagery previously mentioned and data taken by a ground scatterometer system. The major conclusion of these studies was that tillage effect could be quite large (10 dB) below 4 GHz, but could vary with crop type, crop height, radar frequency and incidence angle.

Analysis of airborne scatterometer data taken as a part of the NASA/JSC sponsored Agriculture Soil Moisture Experiment (ASME) in 1978 indicated strong tillage or row effects. The observed magnitude of this effect, 8 dB at 13.3 GHz to 20 dB at 1.6 GHz, and the results of the previous referenced studies established a strong case for a detailed experiment to study the effects of tillage on bare fields, without the variables caused by vegetation and moisture.

A preliminary set of data was gathered over a simulated test site in New Mexico in late 1978. After analysis, the results of this experiment were presented to the ASME team members in early 1979. The team recommended that the experiment be expanded to include different row spacings so a parametric study could be performed. This paper will present the results of data gathered over two simulated field configurations in late 1979.

2.0 EXPERIMENT DESCRIPTION

As stated in the introduction, the object of the experiment was to study the effects of tillage and row spacing on radar backscatter without the variables of moisture and vegetation. To accomplish this, a test site had to be selected in an area where there was minimal rainfall and sparse vegetation. Also, a 50- to 100-acre area had to be made available for controlled test plots.

Agreements were made with the U.S. Department of Agriculture to prepare test plots on the Jornada Experimental Station near Las Cruces, New Mexico. This station is located in an arid area with sparse vegetation and an annual rainfall of 12 inches or less. The soil however, is representative of that found in the central United States.

Two adjacent test plots were prepared as shown in Figure 1. Each plot was 2,500 feet long and 500 feet wide. Simulated rows were plowed across the 2,500-foot dimension on one plot and along the 2,500-foot dimension on the other plot.

Radar backscatter data was gathered by two means. Ground data was gathered by a crane-mounted multifrequency ground scatterometer system. The characteristics of this system are given in Table I. Locations of ground scatterometer data acquisition are shown in Figure 1.

Airborne scatterometer data was gathered using the NASA/JSC C-130 Earth Resources Aircraft. This aircraft carries multiple frequency scatterometer systems with characteristics as described in Table II. The airborne scatterometer data was gathered by multiple flights back and forth across the 2,500-foot length of the test plots.

To establish the electrical and physical characteristics of the fields at the times of radar data acquisition, soil samples and surface profile measurements were obtained. (See Figure 1.) Soil moisture for (0-2) centimeter and (2-5) centimeter depths was obtained from 36 locations in the fields.

The ground scatterometer system was used to acquire radar data for the initial field configuration. Due to the nature of ground scatterometer system data acquisition limitations, several days were required before and after an aircraft flight to obtain enough samples for the data to be meaningful. Only vertically-polarized data was gathered for the initial field configuration.

The major part of the radar data used in this investigation was acquired using the C-130 aircraft scatterometer systems. Two data acquisition flights were conducted, the first on November 16, 1979 and the second on December 11, 1979.

Between these two flights the test-plots configuration was changed as shown in Figure 2. Although it was desired to only have differences in the row-height direction between the measurement times, there was some smoothing of the small-scale roughness evident. The soil moisture remained essentially constant.

Each flight obtained about 20 seconds of radar data for each field at each polarization. In order to determine if the data from the entire field could be averaged, a method was devised to compare the statistics of the data from the fields with those from a reasonably homogeneous scene using the same number of data samples. Some of the statistical data is presented in Table III and Figures 3 through 6.

3.0 RADAR DATA ANALYSES

Data analysis consisted of computation of the mean values of sigma zero for incidence angles over the range of 5 - 50 degrees from aircraft data acquired on November 16, 1979 and December 11, 1979 respectively. This data is presented in Tables IV and V.

For purposes of evaluating the changes in field configuration that were made between November 16, 1979 and December 11, 1979, the along-row and cross-row data were differenced to provide a plot of delta sigma zero ($\Delta\sigma_0$) or modulation function $|M|$. This technique provides an easy means of evaluating changes due to the row structure change. These results are presented in Figures 7 through 10.

Finally, the ground scatterometer data (Table VI) which was acquired over a period of November 14 through November 18, 1979, was differenced and compared to the aircraft data taken on November 16, 1979, (Figure 11). No comparison of the aircraft data taken on December 11, 1979 could be made as no corresponding ground data was taken.

Perhaps a few words about the problems of relating ground scatterometer data to aircraft scatterometer data are in order. There are many variables that must be considered when one tries to relate the two data sets.

First there is the problem of differences in the basic calibraton of the two systems. Each is calibrated by a different method and no technique for cross-checking the two methods has been devised.

Second, there are the interrelated problems of spatial coverage, number of statistically independent samples, measurement time, time for measurement and scene variance. To gather enough statistically independent samples, the ground system must be physically moved to another location. This increases the measurement time, which means the scene can change during the period the measurements are being taken. Lastly, the scene may have natural variances which can effect the data. For instance, data taken on the edge of a field may not be representative of data taken in the center of a field.

For these reasons, the ground scatterometer data was used more for verification of trends rather than comparative sigma zero analysis.

4.0 DISCUSSION OF ANALYSIS RESULTS

In comparing the along-row data taken for both dates, it appears that the small-scale roughness has decreased slightly (Figure 2), which should be expected due to weathering and the deliberate smoothing of the rows. In addition, small differences in the soil moisture, from four percent to five percent, occurred between the measurement dates.

The major differences in the data can be seen in the Modulation Function Curves shown in Figures 7 through 10. The location of the peaks of the modulation functions for November 16, 1979 occur at 25 degrees while their peaks occur at 20 degrees for December 12, 1979. This shift in the peak response corresponds to the measured average row slope change from 26 degrees to 17 degrees. Figures 7 and 9 provide an indication of the frequency sensitivity of the modulation function for bare fields. For the type of field preparation observed, the magnitude of $|M|$ ranged from 5 dB for 13.3 GHz VV to greater than 18 dB for 1.6 GHz VV.

The magnitudes of $|M|$ for either linear polarization (HH or VV) at 4.75 GHz were greater than 12 dB.

Figure 11 is a comparison of the results obtained with the aircraft and ground scatterometer systems for the initial field conditions. The same trends are noted in the data from either system in that $|M|$ peaks at near 25 degrees, the magnitude is frequency-dependent and the shapes of the curves are frequency-independent. The lack of a distinct peak at 25 degrees in the ground data can be attributed to the fact that the ground system only gathers data every ten degrees. In addition, the results show that the method of acquisition of the radar data does not effect the phenomenon observed.

5.0 REPRESENTATIVE MODELS

Several radar backscatter models[4,5,6] applicable to rough surfaces were examined to determine the one which is most applicable to this experiment. The Facet Model, proposed by Khamsi, Fung, and Ulaby[7], provided scene descriptors most applicable for a comparison with the radar data obtained.

This Facet Model describes the scene as a collection of facets of different sizes with Gaussian size and slope distributions. The facets are categorized in terms of their dimensions (ℓ) relative to the observing radar wavelength (λ) as follows:

Large Facets: $\ell > \lambda$

Small Facets: $\ell < 0.4\,\lambda$

Medium Facets: $\lambda > \ell > 0.4\,\lambda$

The scene parameters that drive the model response are the dielectric constant, the facet size standard deviation ($S\ell$), slope standard deviation in the x direction (S_x) and slope standard deviation in the y direction (S_y).

The radar return is defined as the sum of the radar returns due to each facet size. This can be written as:

$$\sigma_0(\theta) = \sigma_{0_L}(\theta) + \sigma_{0_M}(\theta) + \sigma_{0_S}(\theta) \qquad (1)$$

where:

$\sigma_{0_L}(\theta)$ return due to large facets

$\sigma_{0_M}(\theta)$ return due to medium facets

$\sigma_{0_S}(\theta)$ return to small facets.

Near normal incidence, the major part of the return is due to large facets but at larger incidence angles, the medium facets are the major contributor for HH polarization and the small facets are the major contributor for VV polarization.

The look direction modulation function $|M|$ as defined by Ulaby and Bare[3] is:

$$M_{dB} = \sigma_{0_\perp}(dB) - \sigma_{0_{||}}(dB) \qquad (2)$$

where:

$\sigma_{0_\perp}$ (dB) and $\sigma_{0_{||}}$ (dB) are measured with the radar looking perpendicular and parallel to the row direction, respectively. Since the model deals only with the slope distributions about a zero mean slope and the scenes that produce the modulation function have in addition to the zero mean slope distribution at nadir, another slope distribution at the normal incidence to the row slopes, some modifications to the model are needed. In taking a simple approach we have assumed that the slope distribution at the normal incidence to the mean row slope and the nadir slope distributions are the same.

In addition, it is assumed that the large facet returns from each of the two slope distributions combined independently. Thus equation (1) can be expressed as:

$$\sigma_0(\theta) = \sigma_{0_L}(\theta \text{ near } 0°) + \sigma_{0_L}(\theta \text{ near } \theta_s) + \sigma_{0_M} + \sigma_{0_S} \quad (3)$$

where:

σ_{0_L} (θ near 0°) - return due to large facets with mean slope zero

σ_{0_L} (θ near θ_s) - return due to large facets with mean slope = $\tan\theta_s$

Now, combining (2) and (3) we get:

$$M(dB) = \sigma_{0_L}(\theta \text{ near } \theta_s) \quad (4)$$

which implies that the modulation function is a description of the slope distributions S_x and S_y of the scene.

Assuming that the simplifications previously defined are valid, an attempt was made to compare the Facet Model with measured data. Unfortunately, the data given in Reference 7 was derived at a frequency of 9 GHz. If an adequate computer program had been available, sigma zero values corresponding to the test plots could have been derived for each frequency. Since the intent of this effort was to show only that the model did indeed predict the row effects, it was considered acceptable to compare the measured data to predicted data at 9 GHz.

To obtain a prediction of the radar backscatter coefficient using the described model, the statistical descriptors of the roughness, the mean slope of the rows, the distributions of the slopes and the soil moisture at the test plots were required. The following was obtained from the November 16, 1979 data flight, as shown in Figure 2.

Soil moisture - 4%

Mean slope of rows - 26.9°

Small scale roughness - 1 cm

Large scale roughness - 9 cm

Assuming the row structure can be represented by a sinusoid, the standard deviation in the x direction (S_x) is approximately 0.8.

A value of standard deviation in the y direction of 0.1 is assumed to be reasonable. From the values of small scale and large scale rms roughness, a value for the standard deviation of the facet's lengths for the total distribution is approximately 3.14 cm.

Applying these test-plot parameters to the Facet Model data, Figures 27 through 31 of Reference 7 were used to derive 9 GHz sigma zero (σ_0) and modulation function $|M|$ data given in Table VII.

To make a comparison of measured and predicted data, certain criteria of roughness distribution (small, medium, and large) had to be met in the measured data set selected for comparison. Table VIII shows the measured statistical roughness at the Jornada Test Plots and the selection criteria for all four frequencies.

From Table VIII it can be seen that only the 4.75 GHz data set has an allowable facet size spread which matches the criteria used to derive the 9 GHz data.

A comparison of the values of the modulation function derived from the model at 9 GHz and those obtained from the aircraft 4.75 GHz VV scatterometer radar data, is shown in Figure 12.

6.0 EFFECT OF ASPECT ANGLE ON THE SIGMA ZERO OF ACROSS ROW VIEWING

Variations in radar scattering coefficient due to other than orthogonal viewing of row structures (aspect angle) were noted in several of the aircraft data sets. Figure 13 is a two-frequency time history of sigma zero at 20 degrees over a cross-plowed test plot. Also plotted are variations of the viewing angle from orthogonal caused by aircraft heading variations. This figure illustrates the sensitivity of sigma zero to aspect angle for an incidence angle of 20 degrees. Both sigma zero time histories shown have peaks at orthogonal viewing and lower values at the maximum aspect angle (3.5 degrees) encountered during this run.

The observing radars have different antenna beamwidths, eight degrees for the 1.6 GHz system and four degrees for the 4.75 GHz system. This difference is reflected in less sensitivity for the 1.6 GHz system to aspect-angle change when viewing the same scene. In this case, a 3.5 degree change in aspect angle gave a 3 dB change in the 1.6 GHz data and a 6 dB change in the 4.75 data.

7.0 CONCLUSIONS

Several conclusions were drawn from this study. The most significant are as follows:

1. Row direction is a significant contributor to radar backscatter from cropland and must be considered when making radar measurements over bare or sparsely vegetated fields.

2. While the effect decreases with increasing frequency, it is still large (5 dB) at 13.3 GHz.

3. Row effects are independent of linear polarization.

4. The row effect phenomena is defineable by an existing model (Facet Model, Reference 7).

5. There is a strong aspect-angle sensitivity which is a function of the scene and radar system parameters.

8.0 ACKNOWLEDGEMENTS

The authors would like to acknowledge the efforts of the Physical Science Laboratory, New Mexico State University, Las Cruces, New Mexico, for soil moisture sample analysis. Also the Calibration Division of the U.S. Army, White Sands Missile Range, New Mexico for performing soil dielectric properties analysis.

REFERENCES

1. Porcello, L. T.; and Rendleman, R. A.: "Multispectral Imaging Radar." 4th Annual Earth Resources Program Review - Section 35, January 1972.

2. Batlivala, P. R.; and Ulaby, F. T.: "Radar Look Direction and Row Crops." Photogrammetric Engineering and Remote Sensing, vol. 42, no. 2, February 1976.

3. Ulaby, F. T.; and Bare, J. E.: "Look Direction Modulation Function of the Radar Backscatter Coeffic[illegible]icultural Fields." Remote Sensing Laboratory Techn[illegible]ndum 360-3, University of Kansas, Center for Research, Inc., October 1978.

4. Barrick, D. E.: "Rough Surface Scattering Based on the Specular Point Theory." IEEE Trans. on Antennas and Propagation, vol. 16, no. 4, July 1978.

5. Kodias, R. D.: "A Note on the Theory of Scattering from an Irregular Surface." IEEE Trans. on Antennas and Propagation, vol. 14, no. 1, January 1966.

6. Rice, S. O.: "Reflection of Electromagnetic Waves from Slightly Rough Surfaces." Commun. Pure Appl. Math., vol. IV, pp. 351-378, 1951.

7. Khamsi, H. R.; Fung, A. K.; and Ulaby, F. T.: "Rough Surface Scattering Band on Facet Model." Remote Sensing Laboratory Technical Report 177-52, University of Kansas Center for Research, Inc., November 1974.

TABLE I.— NASA/JSC GROUND SCATTEROMETER SYSTEM PARAMETERS

PARAMETERS	K_u	C	L
Frequency (GHz) (f_c)	13.3	4.75	1.6
Polarization	VV	VV, HH, Cross	VV, HH Cross
Along-Track Beamwidth	7.0°	3.0°	8.4°
Cross-Track Beamwidth	8.0°	2.6°	7.7°
Incidence Angles	10°-60°	10°-60°	10°-60°
Bandwidth Sweep	f_c±500 MHz	f_c±500 MHz	f_c±500 MHz
Integration Time	1/300 sec	1/300 sec	1/300 sec
Signal Bandwidth (Hz)			
(θ = 30°)	2975	1150	3700

TABLE I.— NASA/JSC GROUND SCATTEROMETER SYSTEM PARAMETERS

PARAMETERS	K_u	C	L
Frequency (GHz) (f_c)	13.3	4.75	1.6
Polarization	VV	VV, HH, Cross	VV, HH Cross
Along-Track Beamwidth	7.0°	3.0°	8.4°
Cross-Track Beamwidth	8.0°	2.6°	7.7°
Incidence Angles	10°-60°	10°-60°	10°-60°
Bandwidth Sweep	f_c±500 MHz	f_c±500 MHz	f_c±500 MHz
Integration Time	1/300 sec	1/300 sec	1/300 sec
Signal Bandwidth (Hz)			
(θ = 30°)	2975	1150	3700

ORIGINAL PAGE IS
OF POOR QUALITY

TABLE II.— NASA/JSC C-130 AIRCRAFT SCATTEROMETER SYSTEMS PARAMETERS

PARAMETERS	K_u	C	L
Frequency (GHz)	13.3	4.75	1.6
Polarization	VV	VV or HH and Cross	VV or HH and Cross
Along-Track Resolution	120 ft.	120 ft.	120 ft.
Cross-Track Beamwidth	2.5°	4°	8°
Incidence Angles (°)	5 - 50	5 - 50	5 - 50
Nominal Bandwidth (Hz) (θ = 30° Vel = 150 kts)	400	150	50
Nominal Integration Time per Measurement (sec)	0.16	0.32	0.64
Number of Measurements Averaged per Second	6	3	1.5
Precision of Measurement per Second of Spatial Data (dB) (θ = 30°)	+0.36 −0.38	+0.57 −0.62	+1.0 −1.1

TABLE III.— 90-PERCENT CONFIDENCE INTERVAL (dB) FOR AIRCRAFT SCATTEROMETER DATA

Freq. GHz	Polari-zation	Row Direction	Incidence Angle (degrees)									
			5	10	15	20	25	30	35	40	45	50
13.3	VV	Along	3.8	1.8	1.4	1.6	1.6	2.5	2.4	1.8	2.6	2.4
13.3	VV	Across	2.4	1.3	1.2	1.8	2.1	2.3	2.5	1.3	2.1	2.3
4.75	VV	Along	3.7	1.6	2.0	2.5	2.7	2.1	3.0	1.7	3.4	2.8
4.75	VV	Across	2.4	1.5	1.8	1.5	3.1	3.1	2.3	1.9	2.2	3.2
4.75	HH	Along	3.0	2.0	1.7	1.8	2.3	2.0	2.2	2.1	2.9	4.2
4.75	HH	Across	2.7	3.2	3.7	4.3	3.0	4.1	3.0	2.0	2.0	4.0
1.6	VV	Along	3.0	1.5	2.4	2.2	2.1	2.2	3.3	2.6	3.2	4.2
1.6	VV	Across	3.9	2.8	2.2	2.3	2.6	2.8	3.8	3.2	4.6	5.6
1.6	HH	Along	2.8	2.8	1.8	2.7	2.2	3.0	2.7	2.4	2.2	3.1
1.6	HH	Across	4.5	3.4	3.1	2.6	4.1	3.3	4.2	4.2	4.2	3.2

TABLE IV.– MEAN SIGMA ZERO (dB) FOR 13.3 GHz VV, 4.75 GHz VV and HH and 1.6 GHz VV and HH
(Flight Date November 16, 1979)

Freq. GHz	Polarization	Row Direction	Incidence Angle (degrees)									
			5	10	15	20	25	30	35	40	45	50
13.3	VV	Along	-2.6	-6.1	- 8.0	- 9.6	-10.3	-10.8	-11.8	-12.5	-13.1	-13.5
13.3	VV	Across	-1.2	-3.4	- 4.4	- 5.0	- 4.7	- 6.2	- 9.1	-10.6	-11.7	-12.4
		M (dB)	+1.4	+2.7	+ 3.6	+ 4.6	+ 5.6	+ 4.6	+ 2.7	+ 1.9	+ 1.4	+ 1.1
4.75	VV	Along	+4.2	-9.5	-12.4	-14.2	-15.8	-17.4	-18.8	-20.6	-20.9	-22.3
4.75	VV	Across	+4.8	-3.0	- 3.6	- 3.0	- 2.2	- 5.5	-10.9	-17.1	-19.6	-22.7
		M (dB)	+0.6	+6.5	+ 8.8	+11.2	+13.6	+11.9	+ 7.9	+ 2.5	+ 1.3	- 0.4
4.75	HH	Along	-5.0	-12.0	-15.6	-17.2	-18.7	-19.8	-20.8	-21.4	-21.9	-21.6
4.75	HH	Across	-1.5	-5.8	- 7.6	- 7.9	- 7.8	-10.9	-15.5	-18.0	-20.0	-21.0
		M (dB)	+3.5	+6.2	+ 8.0	+ 9.3	+10.9	+ 8.9	+ 5.3	+ 3.4	+ 1.9	+ 0.6
1.6	VV	Along	-4.7	-11.0	-15.5	-18.4	-21.4	-22.3	-21.6	-23.4	-24.8	-24.5
1.6	VV	Across	+3.6	- 2.0	- 2.7	- 2.0	- 3.0	- 6.5	- 7.8	-13.7	-18.3	-19.5
		M (dB)	+8.3	+ 9.0	+12.8	+16.4	+18.4	+15.8	+13.8	+ 9.7	+ 6.5	+ 5.0
1.6	HH	Along	-9.8	-11.7	-14.8	-16.4	-18.6	-20.8	-20.9	-21.0	-25.0	-25.8
1.6	HH	Across	+2.1	- 0.5	- 1.0	- 0.5	- 1.6	- 5.8	- 8.5	-14.5	-18.0	-21.4
		M (dB)	+12.1	+11.2	+13.8	+15.9	+17.0	+15.0	+12.4	+ 6.5	+ 7.0	+ 4.4

TABLE V.— MEAN SIGMA ZERO (dB) FOR 13.3 GHz VV, 4.75 VV & HH, 1.6 GHz VV & HH

(Flight Date December 11, 1979)

Freq. GHz	Polari-zation	Row Direction	Incidence Angle (degrees)									
			5	10	15	20	25	30	35	40	45	50
13.3	VV	Along	-4.4	-6.9	-8.7	-10.7	-11.4	-12.2	-13.2	-14.2	-15.0	-16.1
13.3	VV	Across	-2.0	-3.2	-4.4	-5.7	-7.0	-8.2	-9.5	-11.2	-12.4	-13.1
		M (dB)	+2.4	+3.7	+4.3	+5.0	+4.4	+4.0	+3.7	+3.0	+2.6	+2.4
4.75	VV	Along	+2.0	-11.1	-14.8	-17.8	-18.2	-20.3	-22.0	-23.8	-24.0	-23.5
4.75		Across	+7.8	+1.0	-1.5	-3.9	-4.8	-9.8	-14.4	-19.2	-19.4	-21.1
		M (dB)	+5.8	+12.1	+13.3	+13.9	+13.4	+10.5	+5.6	+4.6	+4.6	+2.4
4.75	HH	Along	-8.6	-15.2	-19.5	-20.8	-21.8	-22.4	-24.5	-25.7	-26.7	-25.2
4.75		Across	-3.0	-6.0	-7.0	-7.4	-7.6	-9.3	-13.4	-18.0	-19.2	-21.3
		M (dB)	+5.6	+9.2	+12.5	+13.4	+14.2	+13.1	+11.1	+7.7	+4.8	+4.4
1.6	VV	Along	-2.1	-7.5	-14.0	-19.5	-20.6	-20.9	-21.5	-22.4	-24.0	-24.8
1.6	VV	Across	+4.3	+1.5	-2.5	-5.4	-9.2	-12.1	-13.3	-16.1	-17.7	-19.4
		M (dB)	+6.4	+9.0	+11.5	+14.1	+11.4	+8.8	+7.2	+6.3	+6.3	+5.4
1.6	HH	Along	-6.0	-12.4	-14.2	-18.2	-18.5	-23.4	-23.4	-26.1	-27.4	-28.1
1.6	HH	Across	+4.6	+2.5	+0.8	-3.4	-3.6	-9.3	-10.0	-14.1	-18.7	-22.6
		M (dB)	+10.6	+14.9	+15.0	+14.8	+14.9	+14.1	+13.4	+12.0	+8.7	+5.5

TABLE VI.— MEAN SIGMA ZERO (dB) FOR 13.3 GHz, 4.75 GHz, and 1.6 GHz GROUND SCATTEROMETER (VERTICAL POLARIZATION)

Frequency (GHz)	Dates	Row Direction	Incidence Angle (degrees)						
			10	15	20	30	40	50	60
13.3	11/14/79, 11/15/79	Along	-6.2	-7.4	-6.5	-7.9	-8.5	-9.7	-12.5
13.3	11/16/79-11/18/79	Across	-2.6	-3.6	-4.7	-4.5	-8.7	-7.4	- 9.0
		M (dB)	+3.6	+3.8	+1.8	+3/4	-0.2	+2.3	+ 3.5
4.75	11/14/79, 11/15/79	Along	-4.9	-7.6	-8.9	-10.1	-11.7	-13.6	-17.0
4.75	11/16/79-11/18/79	Across	-0.6	+0.8	+4.6	+1.3	-13.7	-11.6	-16.4
		M (dB)	+4.3	+6.8	+13.5	+11.4	-2.0	+2.0	+ 0.6
1.6	11/14/79, 11/15/79	Along	-8.5	-11.4	-12.0	-16.2	-16.8	-18.2	-20.2
1.6	11/16/79-11/18/79	Across	+0.5	+2.5	+4.3	+1.6	-9.5	-14.8	-18.1
		M (dB)	+9.0	+13.9	+16.3	+17.8	+7.3	+3.4	+ 2.1

TABLE VII.— VALUES OF MEAN SIGMA ZERO (dB) AT 9 GHz VV DERIVED FROM FIGURES 27 through 31 of REFERENCE 7

Slope Variables	Row Direction	Incidence Angle (degrees)									
		5	10	15	20	25	30	35	40	45	50
CASE I	Along	0	-3.0	-7.6	-13.0	-14.6	-16.0	-16.7	-17.7	-18.1	-18.3
$S_x = 1$	Across	0	-6.8	-2.4	+0.2	+0.2	0	-3.8	-9.3	-18.1	-18.3
$S_y = 0.1$	M (dB)	0	+3.8	+5.2	+13.2	+16.7	+16.0	+12.9	+8.4	0	0
CASE II	Along	-2.1	-3.8	-7.0	-10.4	-14.6	-16.0	-16.7	-17.8	-18.0	-18.4
$S_x = 1$	Across	-1.9	-2.7	-2.9	-2.3	-1.8	-2.8	-4.7	-8.4	-12.5	-15.7
$S_y = 0.15$	M (dB)	+0.2	+1.1	+4.1	+8.1	+12.8	+13.2	+12.0	+9.4	+5.5	+2.7
	$\overline{M}$ (dB)	+0.1	+2.6	+4.7	+11.4	+15.2	+14.8	+12.5	+8.9	+3.6	+1.6

TABLE VIII.— FACET SIZE SELECTION CRITERIA

Facet (ℓ)	Jornada	13.3 GHz	9.0 GHz*	4.75 GHz	1.6 GHz
Size					
Large (cm)	$\ell = 9$	$\ell > 2.25$	$\ell > 3.3$	$\ell > 6.3$	$\ell > 18.75$
Medium (cm)	$\ell = 3$	$0.9<\ell<2.25$	$1.33<\ell<3.3$	$2.5<\ell<6.3$	$7.5<\ell<18.75$
Small (cm)	$\ell = 1$	$\ell < 0.9$	$\ell < 1.3$	$\ell < 2.5$	$\ell < 7.5$

*Derived data

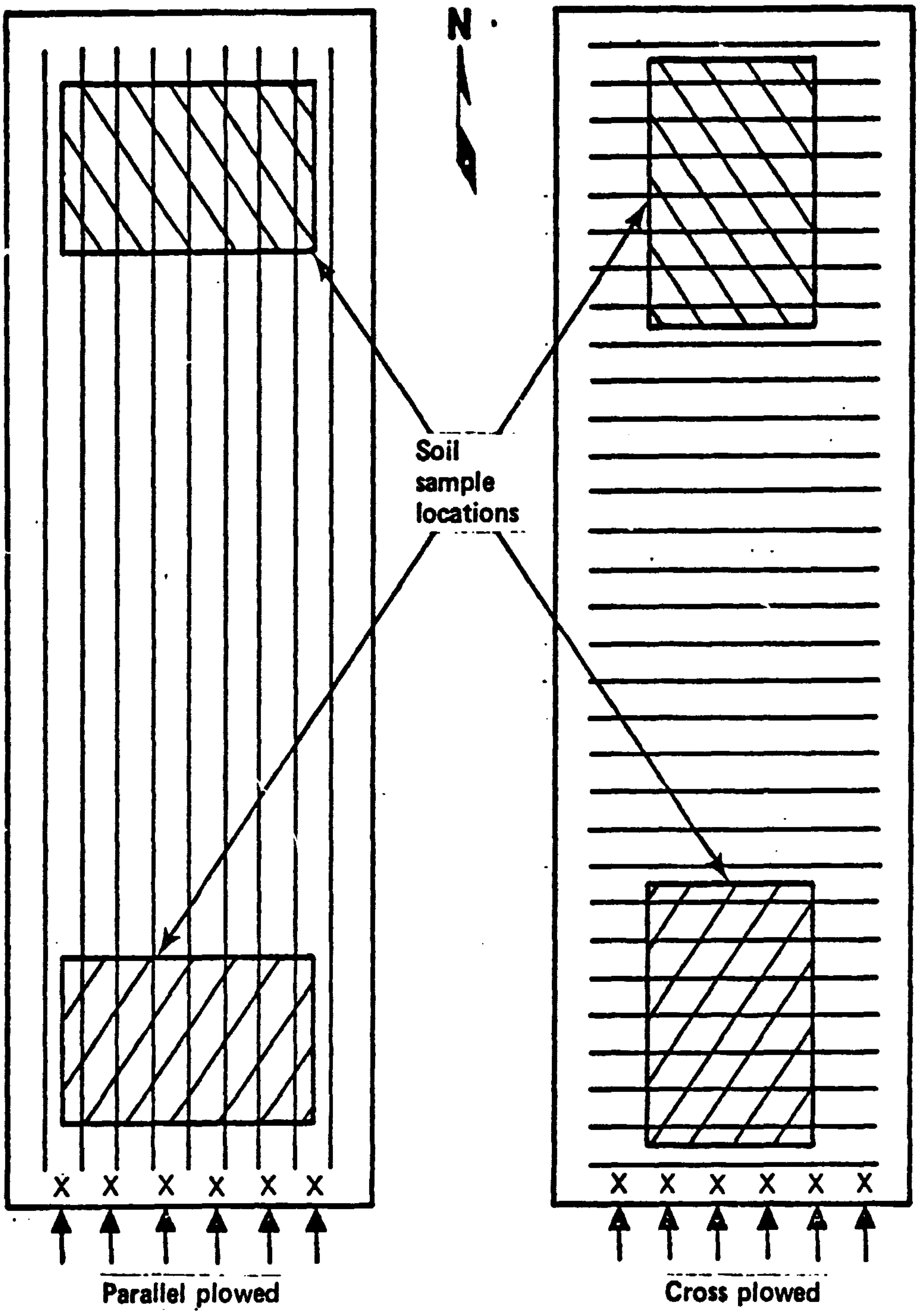

NOTE: X indicates locations for ground scatterometer data acquisition.
↑ indicates direction.

Figure 1.— Ground scatterometer and soil sample locations.

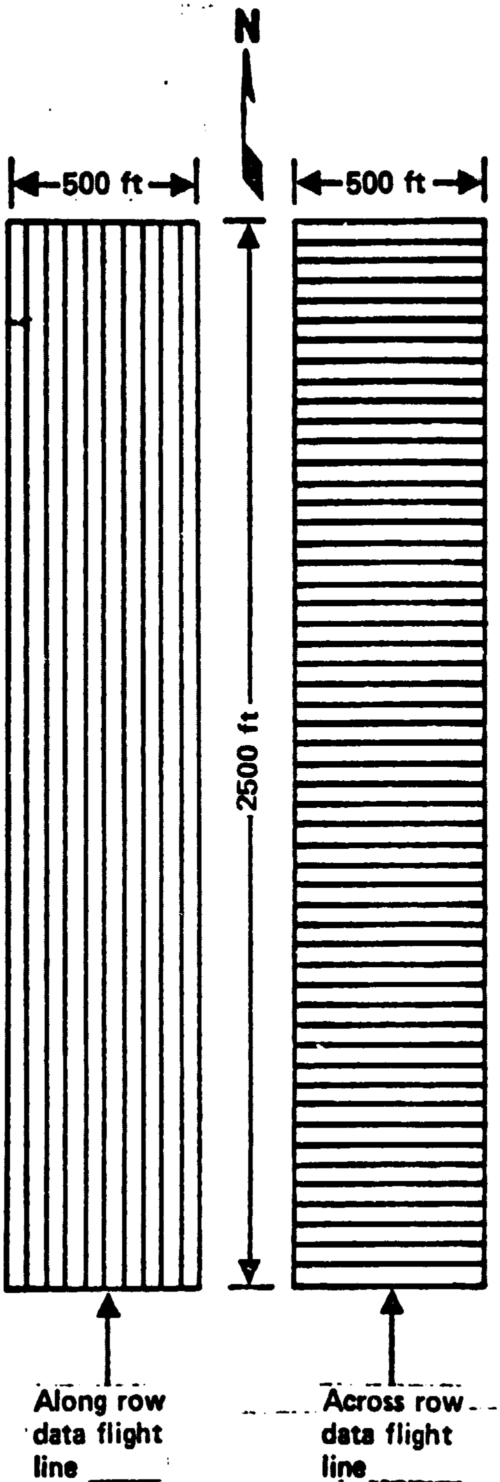

Measurement date	11 16 79
Frequency	13.3 GHz
Polarization	VV
Radar look	Parallel

Measurement date:	11/16/79
Soil moisture:	4 percent by weight
Row spacing:	100 cm
Row height	25.4 cm
RMS small scale roughness:	1 cm
RMS large scale roughness:	9.0 cm

Measurement date:	12/11/79
Soil moisture:	5 percent by weight
Row spacing:	100 cm
Row height:	15 cm
RMS small scale roughness:	0.6 cm
RMS large scale roughness:	6.0 cm

Figure 2.— Test site configuration at times of aircraft data acquisition.

ORIGINAL PAGE IS
OF POOR QUALITY

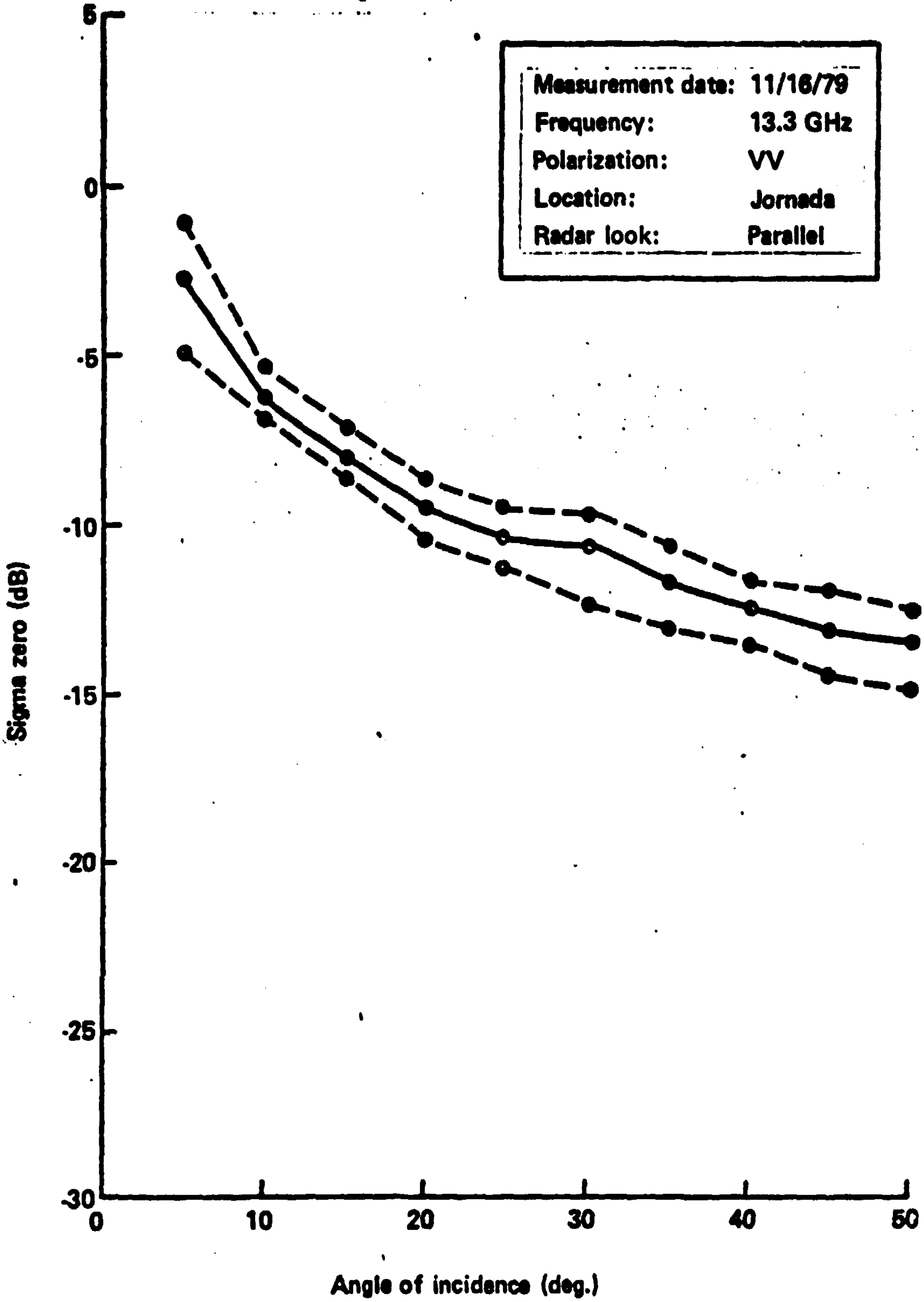

Figure 3.— Mean sigma zero and 90 percent confidence interval versus angle of incidence.

ORIGINAL PAGE IS
OF POOR QUALITY

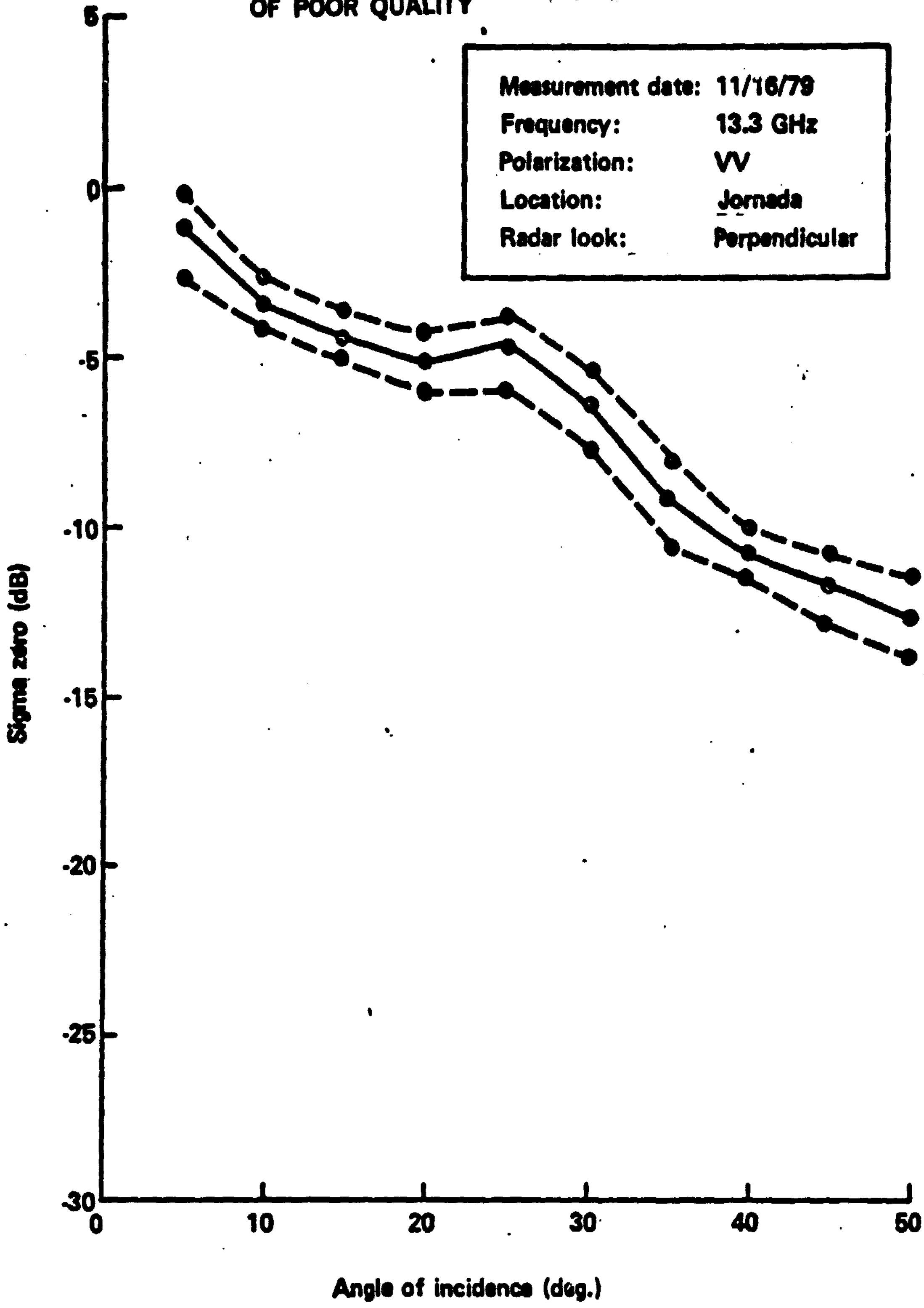

Figure 4.— Mean sigma zero and 90 percent confidence interval versus angle of incidence.

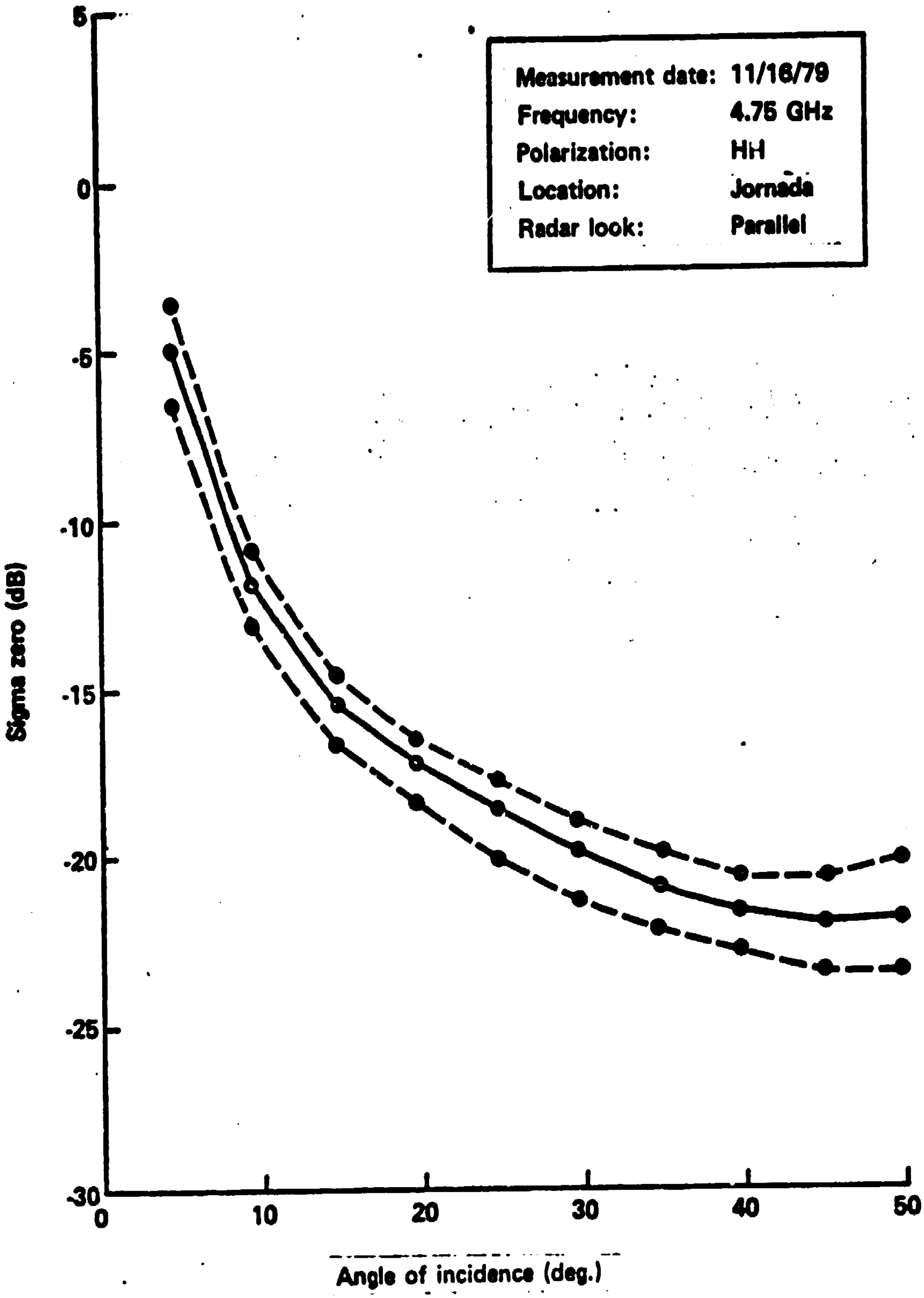

Figure 5.— Mean sigma zero and 90 percent confidence interval versus angle of incidence.

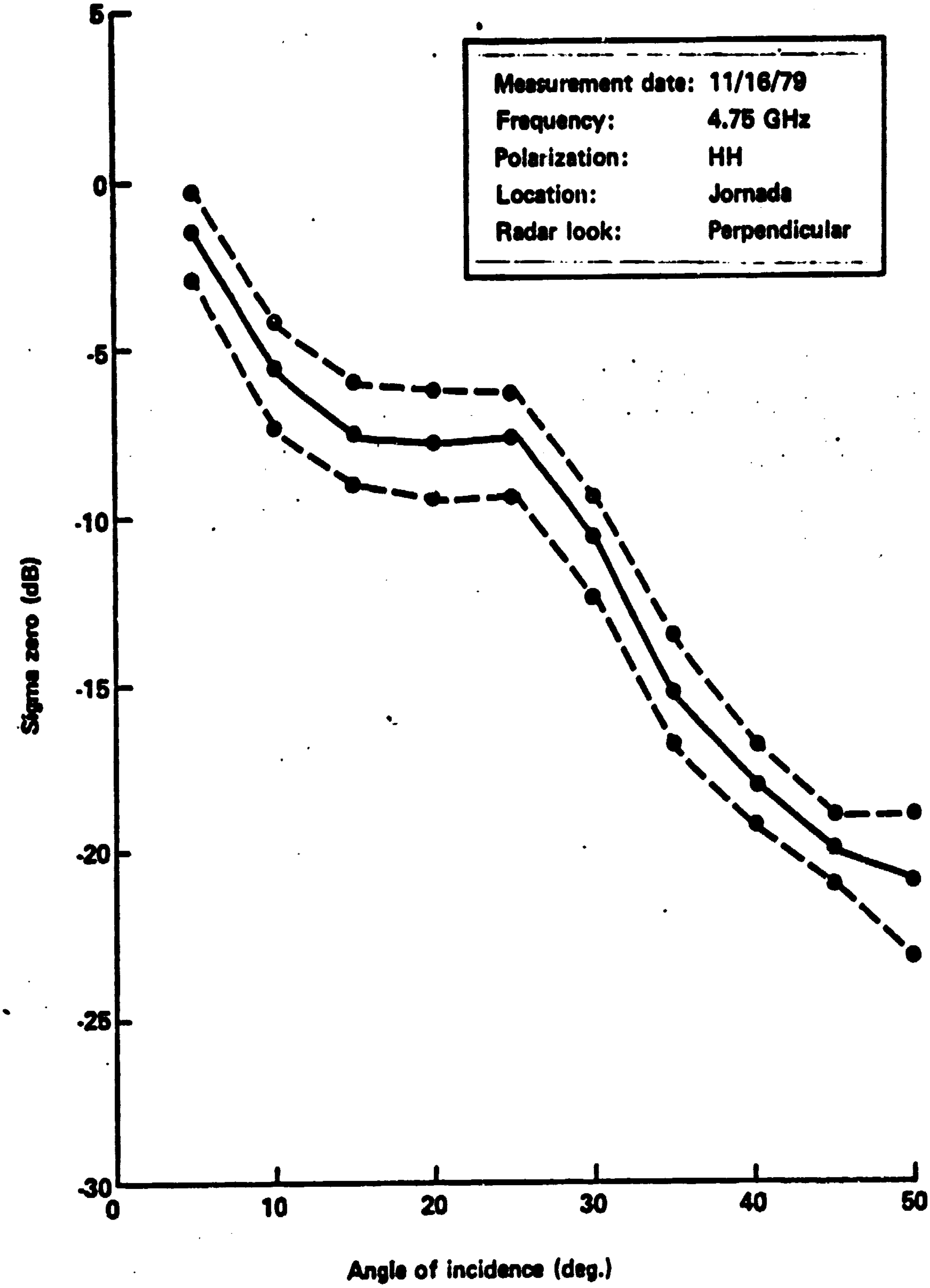

Figure 6.— Mean sigma zero and 90 percent confidence interval versus angle of incidence.

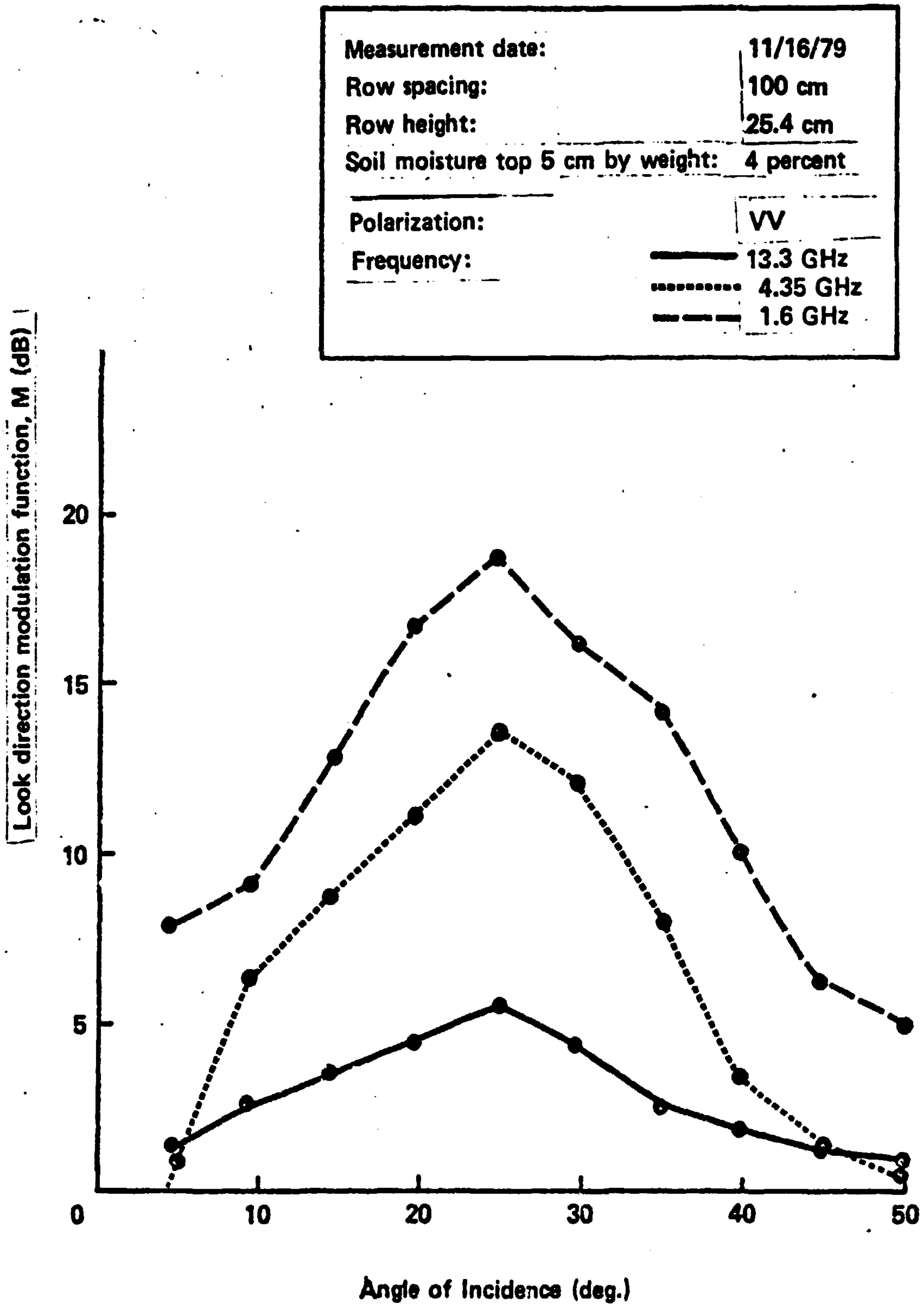

Figure 7.— Comparison of angular response of the modulation function of a bare field for three frequencies.

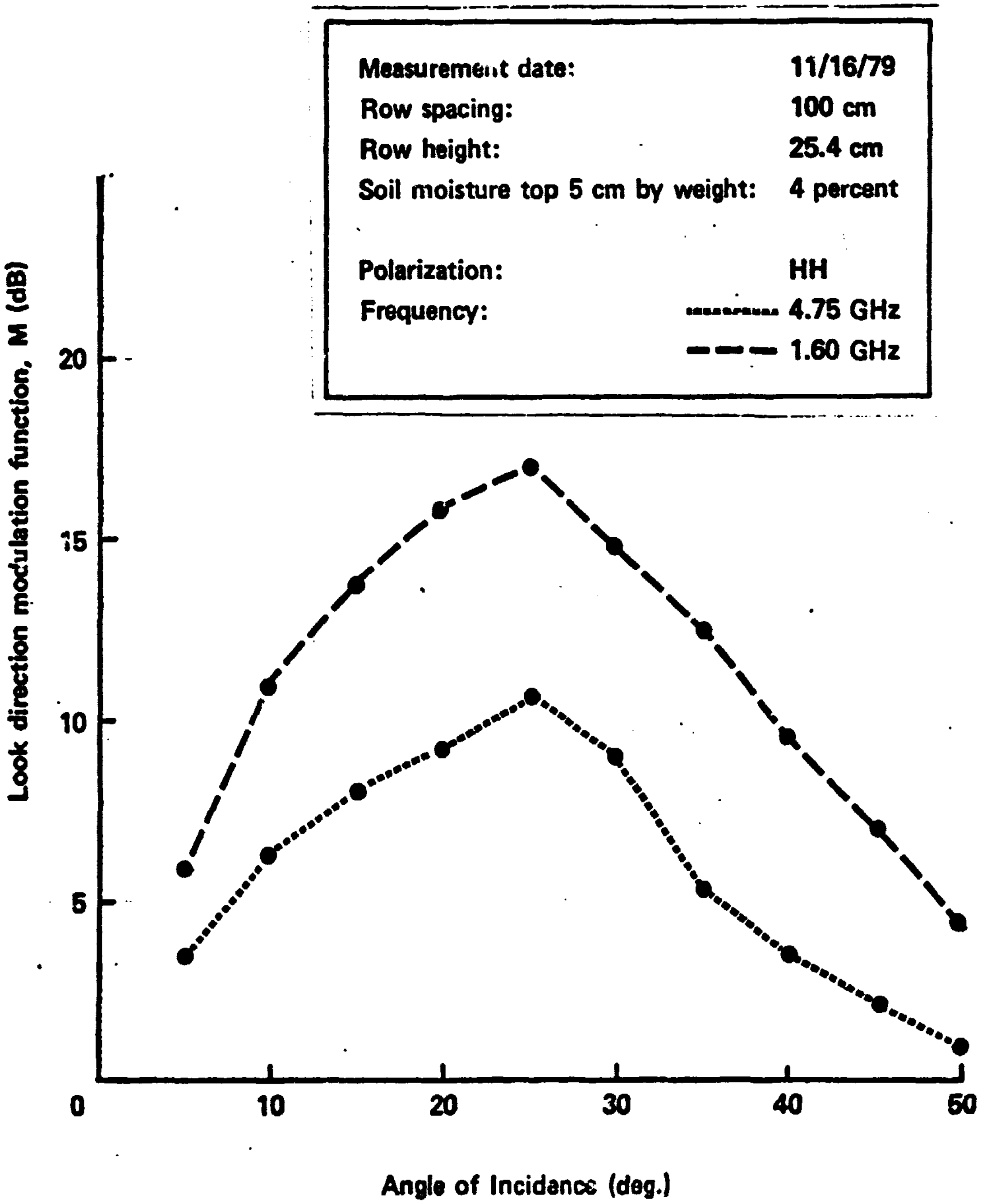

Figure 8 .— Comparison of angular response of the modulation function of a bare field for two frequencies.

ORIGINAL PAGE IS
OF POOR QUALITY

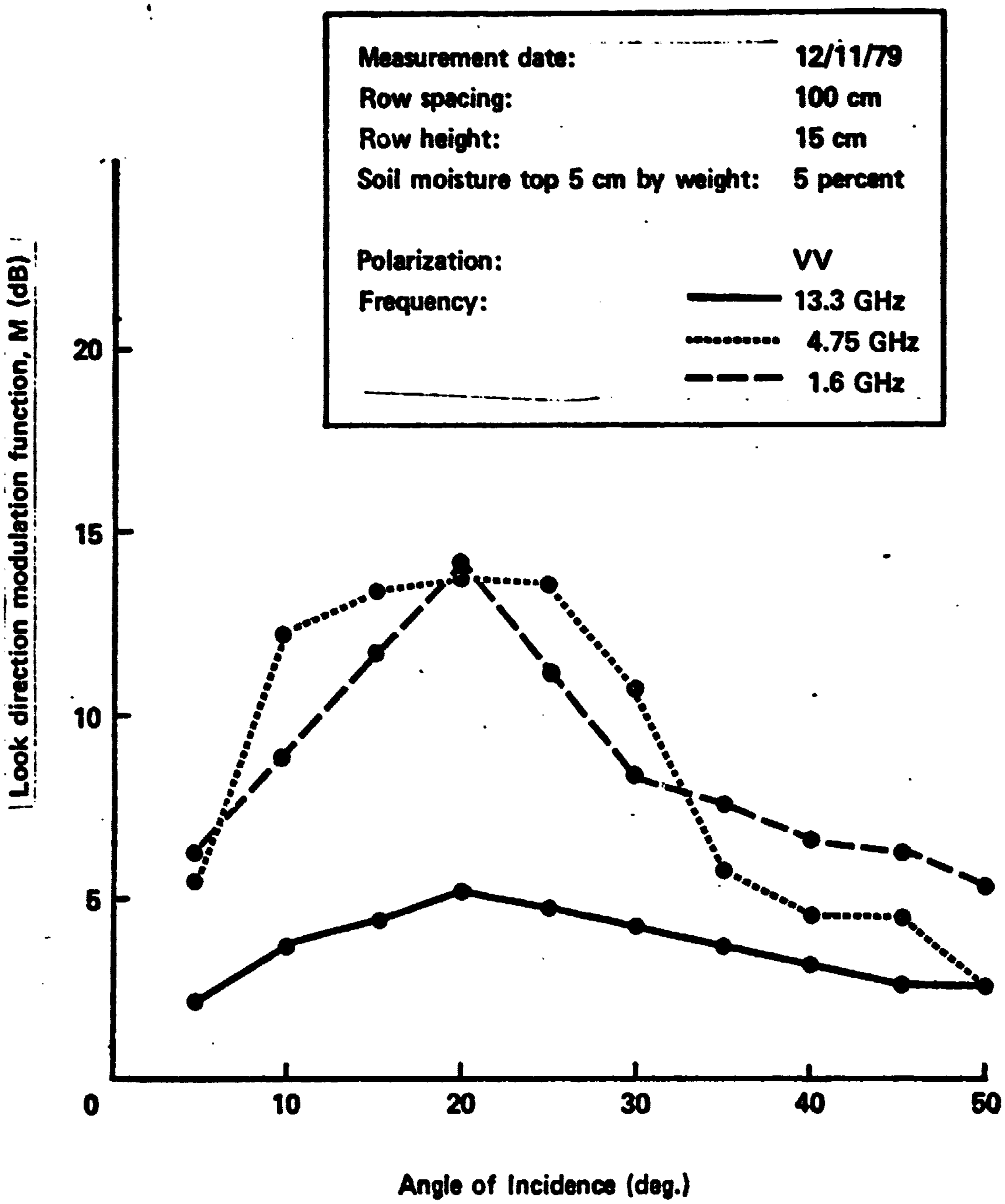

Figure 9 .— Comparison of angular response of the modulation function of a bare field for two frequencies.

ORIGINAL PAGE IS
OF POOR QUALITY

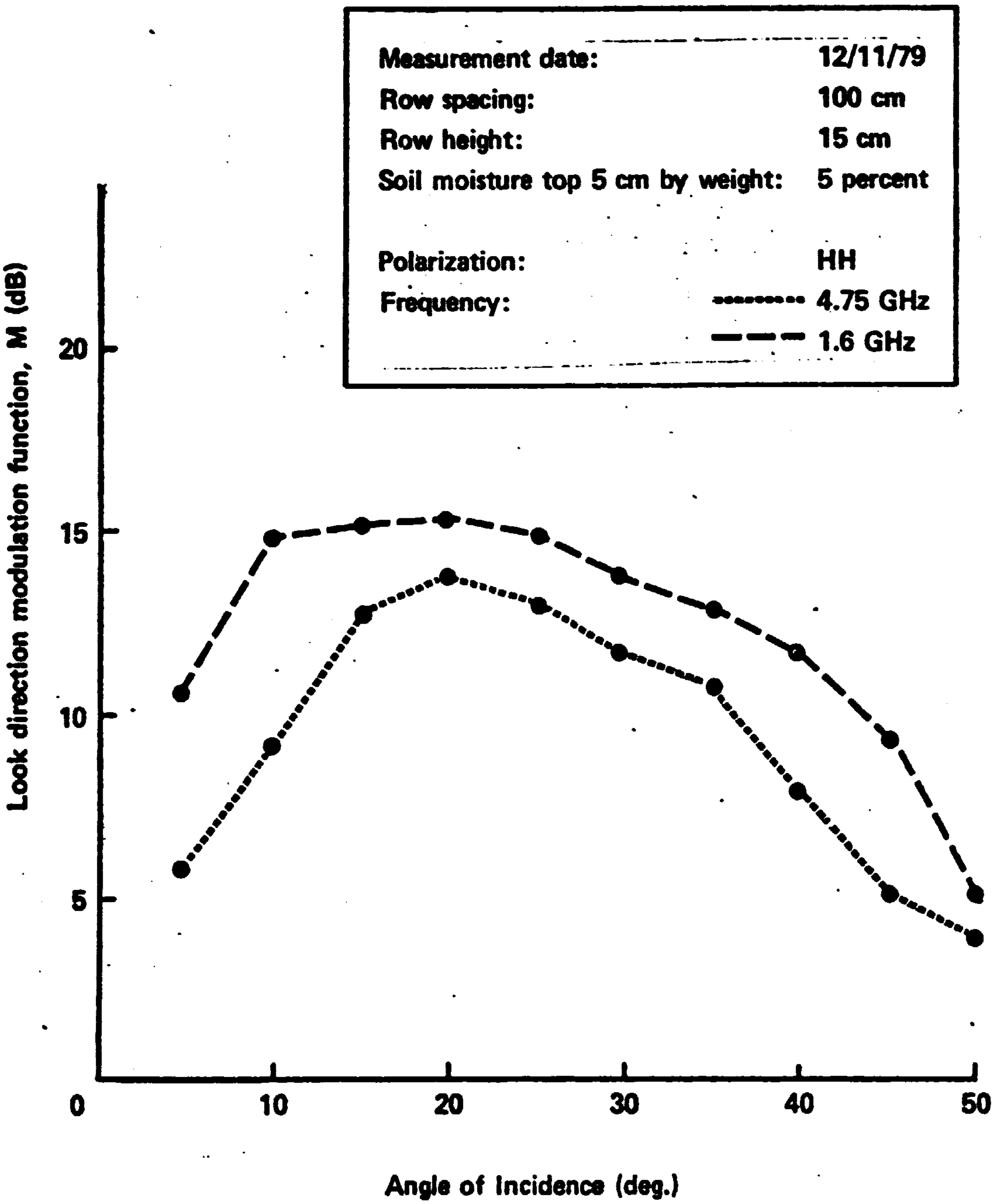

Figure 10.– Comparison of angular response of the modulation function of a bare field for two frequencies.

ORIGINAL PAGE IS
OF POOR QUALITY

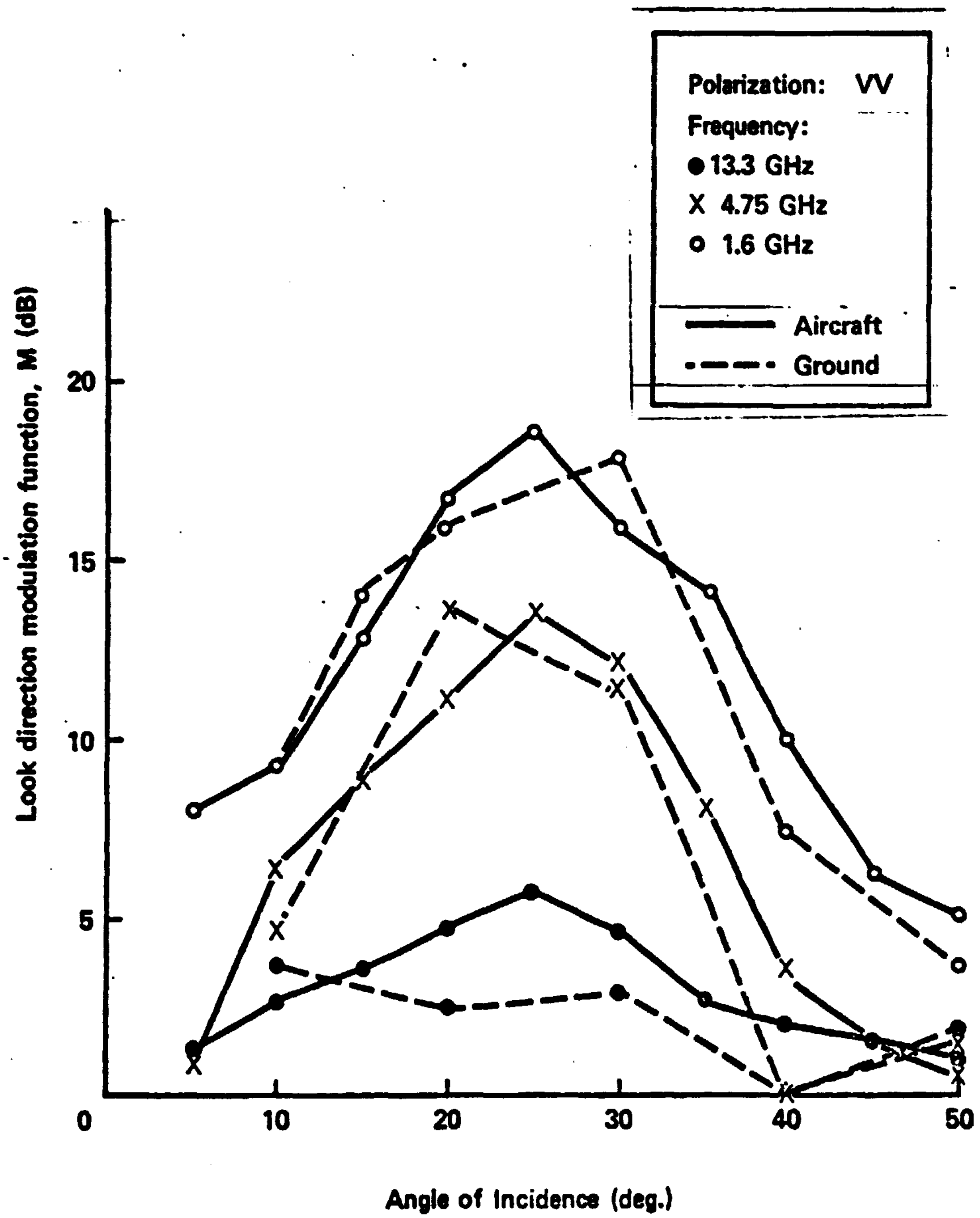

Figure 11.– Comparison of aircraft and ground acquired angular response.

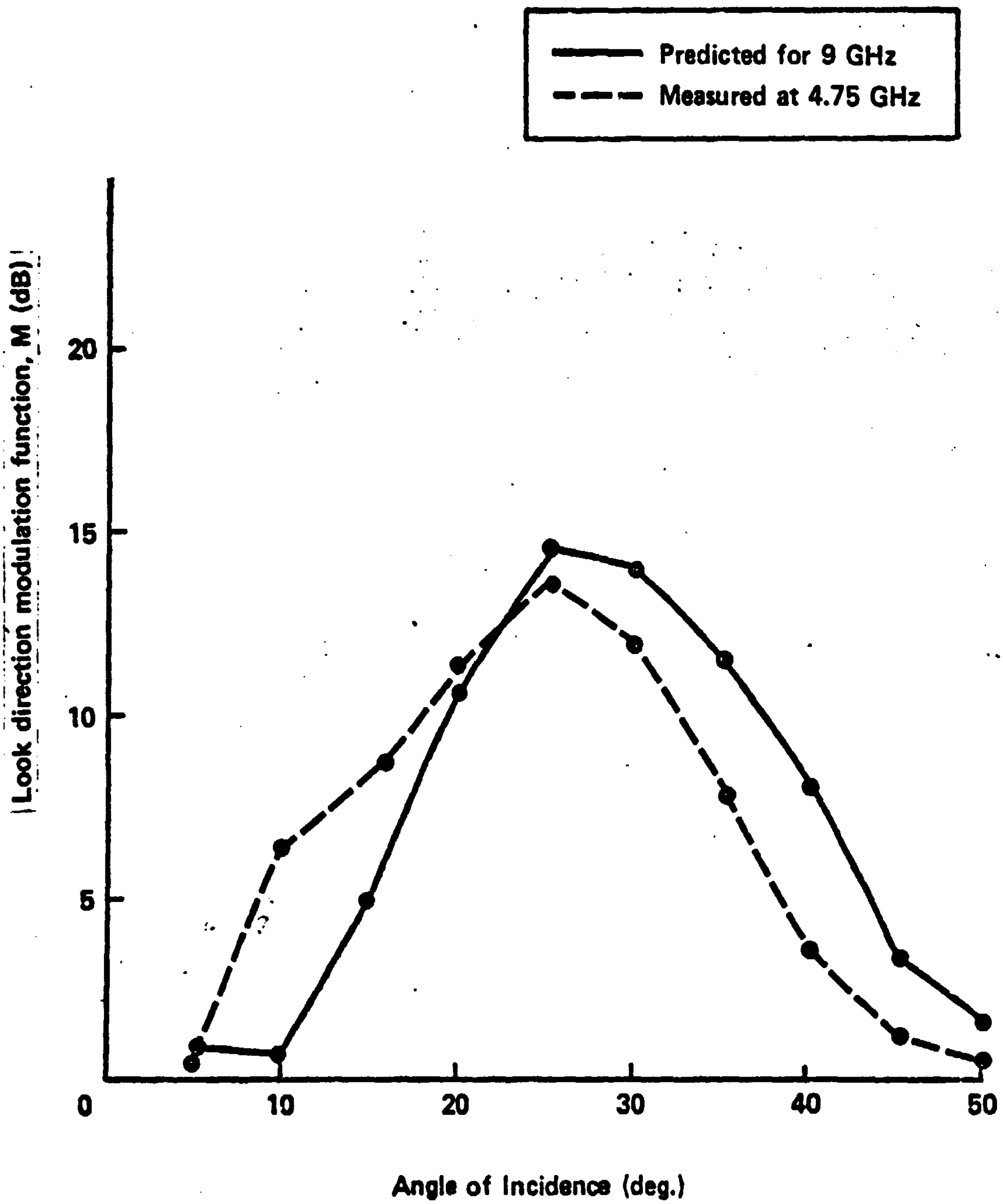

Figure 12.– Comparison of the predicted values of the angular response of the modulation function.

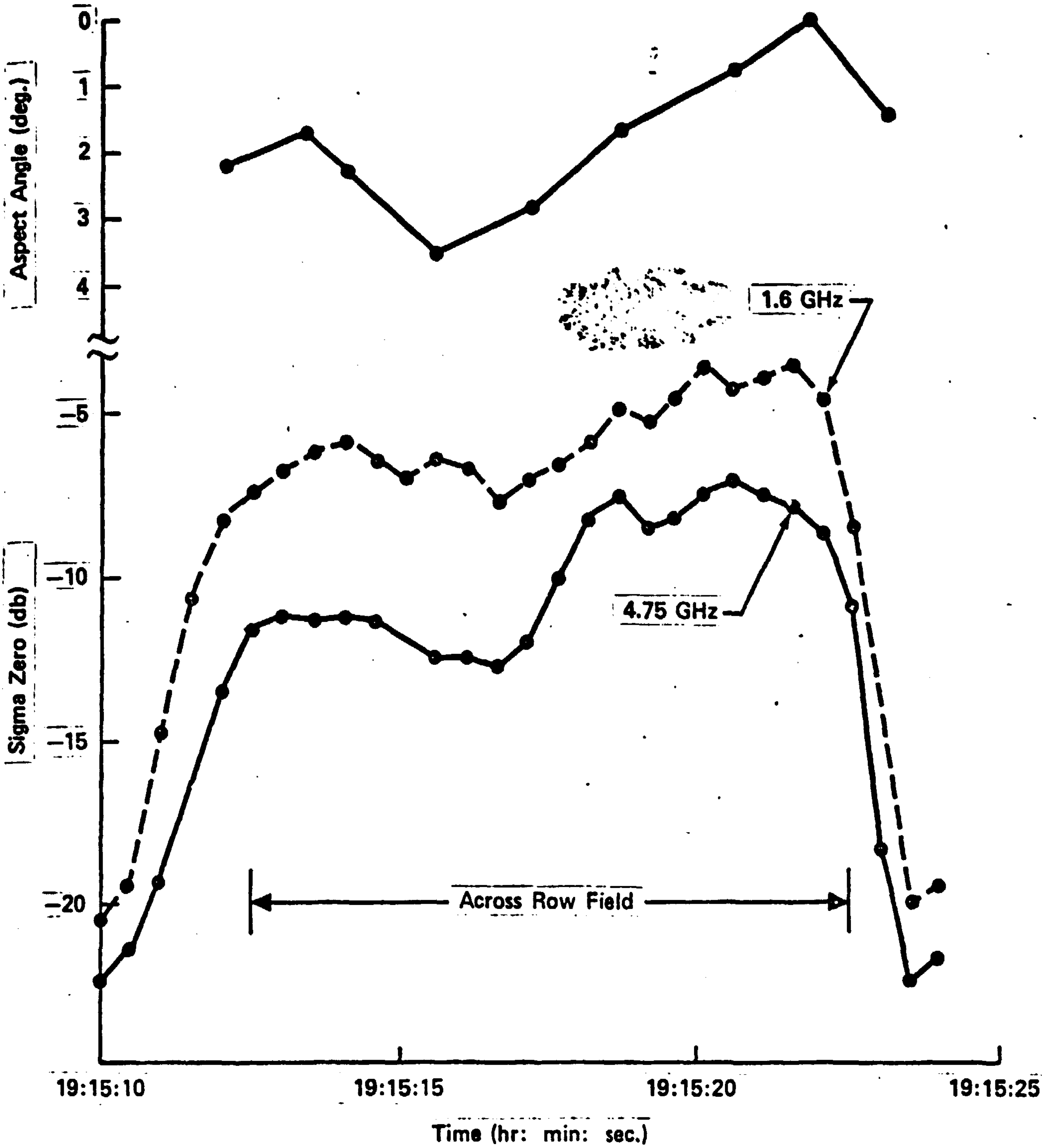

Figure 13.– Time history of 20° incidence angle (4.75 GHz and 1.6 GHz sigma zero) plotted with Aspect Angle.

NASA-JSC